INTERNAL SOLITARY WAVES PHASE SPEED ESTIMATION IN THE LOMBOK STRAIT USING MULTI-SATELLITE DATA

Chonnaniyah*[1], Takahiro Osawa[2] and Abd Rahman As-syakur[3]
[1]Researcher, Environmental Engineering Program, Institute of Sciences and Technology Nahdlatul Ulama Bali, Denpasar, Bali 80119, Indonesia
Email: chonnaniyah@istnuba.ac.id

[2]Professor, Center for Research and Application of Satellite Remote Sensing (YUCARS), Yamaguchi University, Tokiwadai, Ube, Yamaguchi 755-0097, Japan
Email: osawaunu@yamaguchi-u.ac.jp

[3]Researcher, Department of Marine Sciences, Faculty of Marine Science and Fisheries, Udayana University, Jimbaran, Badung, Bali 80361, Indonesia
Email: assyakur@unud.ac.id

KEYWORDS: Internal solitary waves; Lombok Strait; multi-satellite; phase speeds

ABSTRACT: This study used multiple satellites equipped with synthetic aperture radar (SAR) and optical sensors to estimate the phase speeds of internal solitary waves (ISWs) in the Lombok Strait. During the southeast monsoon period, ISW phase speeds in the Lombok Strait were observed using Sentinel-1/SAR, GCOM-C/SGLI, and Terra/MODIS sensors. It is assumed that ISW in the Lombok Strait arises from the interaction between the semidiurnal tides and the coarse bathymetry (sill) in the southern part of the strait. ISW phase speed using multi-satellite data is estimated by dividing the distance between the detected first crest patterns by the time difference between the two images recorded. This study examines multi-satellite data capacity to estimate the Lombok Strait propagation speed. Estimating ISW phase speed derived from multi-satellite images showed that the phase speed was slower when the ISW packet reached the Kangean Island area. The results correlated with the variation of bathymetry along the ISW propagation to the northern part of the strait. The multi-satellite observation data used in this study enhanced our understanding of the influence of bathymetry variation on the estimated phase speeds in the Lombok Strait.

1. INTRODUCTION

Internal solitary waves (ISWs) are non-linear internal waves with large amplitudes that appear as single waves propagating within the ocean. They often generate at interfaces between layers of different densities, such as at the thermocline. Although ISWs are waves in the ocean, they create a surface manifestation that can be detected visually or through remote sensing. These waves are essential in many ways, as they are present wherever there are strong stratification and tides near irregular topography. These waves can extend for several kilometers, have complex shapes, and are isolated (Apel, 2002). Lombok Strait, one of the famous generation sites of ISWs large amplitudes, is a narrow passage between Bali and Lombok's islands in the southern part of the Indonesian seas. Lombok Strait is a pathway to exchange water masses between the Indian and Pacific oceans, resulting in strong tidal currents and complex oceanographic dynamics (Susanto et al., 2005).

Various observational techniques, including in-situ measurements (Purwandana et al., 2021; Syamsudin et al., 2019), numerical simulations (Gong et al., 2022; Ningsih et al., 2008), and remote sensing (Chonnaniyah et al., 2021; Karang et al., 2019; Karang & Nishio, 2011; Matthews et al., 2011; Mitnik et al., 2000; Susanto et al., 2005), have been used to study the manifestation of ISWs in the Lombok Strait. Remote sensing plays a crucial role in studying IWs in the ocean by providing details of the two-dimensional spatial structure, which cannot be easily obtained in situ measurement. These details include an overall characteristic that indicates important properties of ISWs, such as soliton number, wavelengths, propagation directions, and propagation speed. Synthetic Aperture Radar (SAR) is one of the primary satellite instruments used for this purpose, owing to its capability of capturing sea surface manifestations caused by ISWs (Robinson, 2010). Optical sensors on spacecraft can also be used to detect these patterns, but this method is limited to daytime, clear skies, and favorable viewing geometry concerning the position of the Sun (Jackson, 2007).

Satellite images can determine essential parameters of ISWs such as amplitude, wavelength, crest length, width of solitons, number of waves per packet, inter-packet distances, and propagation direction. By analyzing pairs of images captured by different satellite sensors, the speed of ISWs can also be estimated (Chonnaniyah et al., 2021, 2023; Liu et al., 2014; Tensubam et al., 2021). Furthermore, the estimated phase speeds from the surface signatures of ISWs can be utilized to investigate mixed layer depth, stratification, heat content, and changes in the topography of the region (Jackson, 2007). Studying internal waves is challenging since they are unpredictable by nature (Woodson, 2018). However, remote

sensing techniques can offer useful information about the characteristics and movements of ISWs. This type of research helps us understand how ISWs affect oceanic processes, impact coastal areas, and interact with other ocean features. ISWs are a fundamental component of ocean dynamics. Estimating their phase speed helps scientists understand how these waves propagate, interact with other oceanic features, and influence ocean circulation patterns. This knowledge contributes to a better understanding of oceanic processes.

ISW phase speed can be estimated using multi-satellite imagery by comparing a pair of images detecting the same ISW packet at nearly the same time. To determine the speed of ISWs using satellite imagery, a pair of images capturing the same ISW packet at different time intervals is necessary. By utilizing multi-satellite imagery, almost identical time differences can be obtained. Tensubam et al. (2021) employed this technique to estimate the ISW phase speed in the Andaman Sea through three different methods. Their estimations agreed with theoretical results obtained from the Sturm-Liouville equation using monthly climatological stratification data and local bathymetry. The study emphasizes the importance of water depth and monthly stratification in controlling the ISW phase speed in the Andaman Sea.

Previous research by Mitnik and Susanto estimated the ISW phase speed in the Lombok Strait using the distance between packets in one SAR image. Purwandana et al. (2021) also estimated the ISW phase speed in the Lombok Strait, utilizing in-situ data and Himawari imagery, which showed consistent results with the research findings of Susanto et al. (2005). Chonnaniyah et al. (2021) estimated the ISW phase speed in the northern part of the Lombok Strait using Sentinel-1 SAR imagery and Himawari-8 high temporal resolution image. Their estimation results using Sentinel-1 and Himawari-8 imagery were consistent with those using Himawari-8 imagery on the same day with a time difference of 10 minutes. This research added two different optical sensors from Himawari-8/AHI, GCOM-C/SGLI, and Terra/MODIS to enhance the accuracy of ISW detection further. The addition of these sensors aims to reduce the time difference between images that detect ISW patterns on the same day. The research also revealed that the GCOM-C/SGLI and Terra/MODIS image pairs have shorter time differences, improving the precision of ISW phase speed estimation. The research motivation behind estimating internal wave phase speed using multi-satellite images is driven by the need to deepen our knowledge of oceanic processes, enhance predictive capabilities, and address various ecological, climatic, and navigational challenges associated with these waves.

2. DATA AND METHOD

2.1 Data

ISWs can be identified in SAR images by a visible pattern of alternating bright and dark bands (Jackson et al., 2013). Conversely, in sun-glint optical images, the same waves appear as a pattern of dark bands followed by bright bands (Jackson, 2007). The leading wavefront of each wave packet is followed by a trailing wave train. The amplitude of the Bragg waves is enhanced (reduced) in the convergence (divergence) zone created by the ISWs. As a result, the surface roughness increases in the convergence region and decreases in the divergence zone. SAR imagery displays bright patches in rough convergence zones and dark patches in smooth divergence zones, whereas sun-glint optical images show the opposite pattern (Alpers, 2014). Multi-satellite radar and optical images can reveal differences in the patterns of ISWs and the estimated characteristics of ISW dynamics in the Lombok Strait. SAR data has been widely used to estimate and detect the dynamic characteristics of ISWs, as it is the most effective tool for this purpose. In this study, we utilized open-access Sentinel-1 SAR data, which includes day and night C-band SAR imagery. Level-1 Ground Range Detected (GRD) products were employed to detect ISWs in the Lombok Strait. Specifically, the Interferometric Wide swath mode of the Level-1 GRD products covers a wide area of 250 km x 200 km in a single scene. The Interferometric Wide mode has the advantage of combining two sequential scenes to create a more significant research area with linear dimensions of up to 400 km, thereby expanding the scope of the study.

Optical sensors are another type of instrument capable of detecting ISW patterns. They have the advantage of high temporal resolution, although their observations are limited to daylight hours and require cloud-free conditions. This study analyzed ISW patterns using optical images from various instruments, including the Second-generation Global Imager (SGLI) sensor obtained from the Global Change Observation Mission-Climate (GCOM-C), the Moderate Resolution Imaging Spectroradiometer (MODIS) sensor on board the Terra satellite, and the Advanced Himawari Imager (AHI) aboard the Himawari-8. Visible band products were used to observe and estimate detected ISW patterns, which were then compared to SAR images for validation. SGLI is an optical sensor that can observe multiple channels from near ultraviolet to thermal infrared wavelengths. It consists of the Visible and Near Infrared Radiometer (VNR) and the Infrared Scanning Radiometer (IRS). VNR has 11 channels for non-polarized nadir view (VN) and two for polarized/along-track slant view (P). IRS has four short-wavelength infrared channels (SW) and two thermal infrared channels (T). The VNR and IRS have scan widths of 1150 km and 1400 km, respectively (Ogata et al., 2017). MODIS sensor has 36 channels in the range of visible and infrared regions with a spatial resolution of about 250 m and 1 km, the spectrum from 0.412μm to 14.235μm. The AHI sensor has 16 observation bands and offers a spatial resolution of 0.5 or 1 km for visible and near-infrared bands and 2 km for infrared bands. The Himawari-8 geostationary satellite has a shortened revisit time of around 10 minutes for Full Disk and 2.5 minutes for sectored regions (Bessho et al., 2016). The selection of satellite data was based on the proximity of optical images detecting ISW patterns that aligned with ISW patterns detected by SAR. Table 1 summarizes the relevant information regarding the satellite data used in this study.

Table 1. Summary of used satellite data

Satellite/ Sensor	Date, Time (hh: mm, local time)	Spatial resolution (m)	Products
Sentinel-1B/ SAR	25 October 2018, 18:25	20	Level-1 Ground Range Detected
GCOM-C/SGLI	26 October 2018, 10:19	250	Visible band (673 nm)
Terra/ MODIS	26 October 2018, 10:25	250	Visible band (645 nm)
Himawari-8/AHI	26 October 2018, 13:40	500	Visible band (640 nm)

The research location is focused on the Lombok Strait area to the northern part approaching Kangean Island (Figure 1a). The depths within the Lombok Strait generally range from 800 to 1000 meters, except for the southern end of the strait, where a shallow sill is present. The strait is divided into two channels at this location by the small Nusa Penida Island. On the eastern side of Nusa Penida Island, there is an irregularly shaped sill connecting Nusa Penida Island with Lombok Island. The sill has a maximum depth of 350 m and extends 20 km (Murray et al., 1990). Sentinel-1B/SAR image was acquired at 18:25 WITA (Central Indonesian Time) on 25 October 2018, showing packets of ISWs propagating northward and southward (Figure 1b).

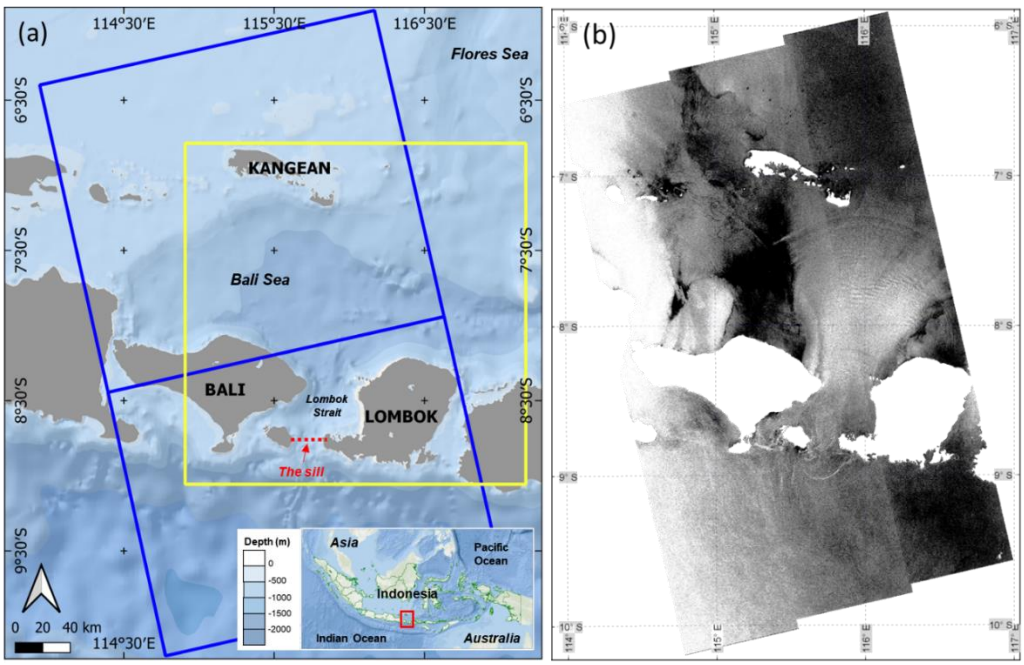

Figure 1. (a) Map of the Lombok Strait bathymetry. Square blue and yellow lines represent the Sentinel-1 SAR image swath for ascending orbit mode and the research location focus, respectively. The red line represents the sill location. (b) Sentinel-1/SAR images with ISW patterns were detected on 25 October 2018 at 18:25 WITA.

In the Lombok Strait, SGLI, MODIS, and AHI sensors captured visible band imagery (at 673 nm, 645 nm, and 640 nm, respectively). In Figure 2(a), the SGLI imagery detected more than 13 solitons in packets near Kangean Island and in the Lombok Strait area more than three solitons. Similarly, Figure 2(b) shows the MODIS imagery where more than 13 solitons were detected in packets near Kangean Island, and more than three solitons were observed in packets within the Lombok Strait area. Figure 2(c) shows that the AHI image detected more than 13 solitons in packets near Kangean Island and more than three solitons in the Lombok Strait area. All the images used in this research focus solely on the southeast monsoon because the water conditions around the Lombok Strait exhibit stronger stratification characteristics than the northwest monsoon (Susanto, Gordon, and Sprintall, 2007).

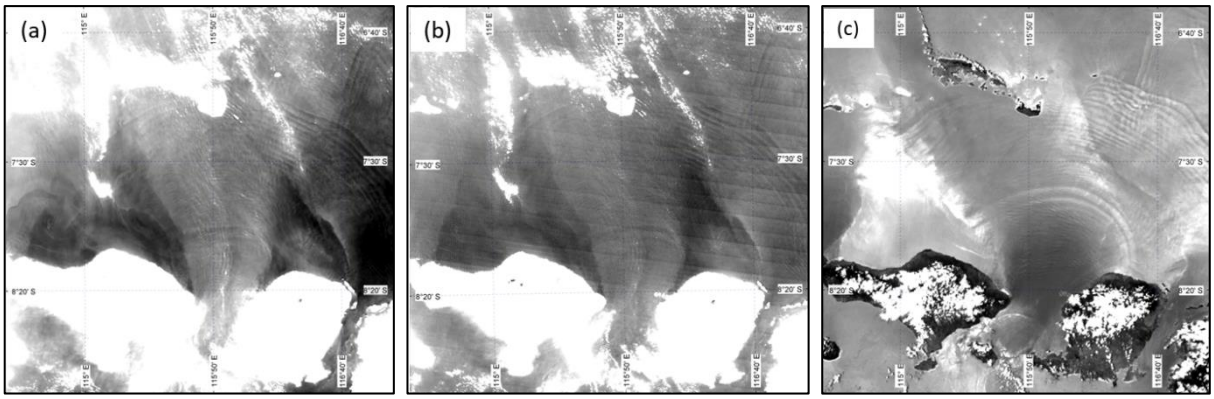

Figure 2. (a) SGLI 673 nm visible band with ISW patterns detected on 26 October 2018 at 10:19 WITA, (b) MODIS 645 nm visible band on 26 October 2018 at 10:25 WITA, and (c) AHI 640 nm visible band on 26 October 2018 at 13:40 WITA.

2.2 Method

SAR and optical images can be used to estimate different parameters of these waves, such as phase speed, wavelength, soliton number, first crest length, and propagation direction. The leading soliton, or the first crest of the soliton in one packet, usually has the brightest intensity. The soliton number is described as several bright/dark lines in one packet. One packet's average wavelength between solitons is the distance between two adjacent bright bands. The ISW phase speed can be estimated using SAR (Sentinel-1) and optical (SGLI, MODIS, and AHI) imagery. Using data from multiple satellites increases the coverage area and duration of observation, allowing for a more comprehensive understanding of internal wave dynamics across different regions and periods. Different satellites may employ distinct sensors and imaging techniques, offering diverse perspectives on the same phenomenon, leading to a more nuanced understanding of internal wave behavior.

ISW phase speed estimation using satellite imagery requires images capturing the same ISW packet at different time intervals. Multi-satellite imagery makes it possible to obtain nearly close time differences. ISW phase speed can be estimated by measuring the displacement of the ISWs packet between successive satellite observations. This displacement represents the wave's distance during a specific time interval. To estimate the phase speed of ISWs, divide the measured displacement by the corresponding time interval. This study measured the distance differences by comparing ISW patterns extracted from optical and SAR images. It was observed that detecting the ISW packet in optical images is more straightforward than in SAR images. The time gap between the SAR and optical images was approximately 15-18 hours, exceeding the semidiurnal tidal period. ISW packet detected in the SAR image is assumed to propagate northward until it approaches Kangean Island, which is subsequently detected in the optical image. Packet 2 cannot be estimated using SAR imagery because no new packet has been generated in the sill area. Therefore, the estimation for Packet 2 focuses on the ISW pattern in the SGLI to MODIS and AHI images. In the northern part of the Lombok Strait, ISW propagation varies within an ISW packet due to differences in depth during propagation. This research estimates the ISW phase speed along five transect lines created to measure the distance of ISW Packets detected by various sensors.

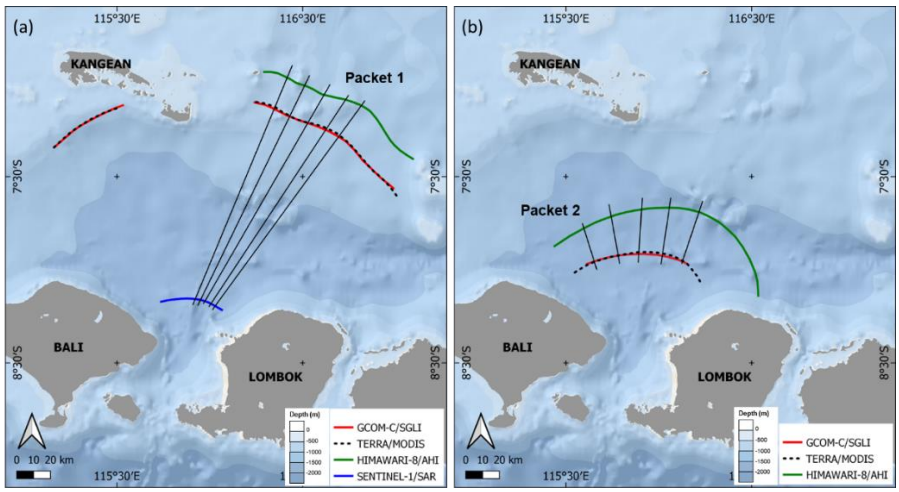

Figure 3. Transect lines for the multi-temporal image method. (a) Packet 1 with the ISW pattern that matches between the optical and SAR images, and (b) Packet 2 with the ISW pattern that has a match only on optical images.

3. RESULTS AND DISCUSSION

Figure 3(a) shows the ISW packet movement detected in four image pairs and the estimated ISW phase speeds using multi-satellite focused on SAR image. The movement of the ISW packet detected in four image pairs along with the estimated ISW phase speeds, using multi-satellite focused on SAR image. The solid red curve represents SGLI, the dashed black curve represents MODIS, and the solid green curve represents AHI. These optical images show the depth of the waters around the ISW pattern extraction to be around 500 m. Conversely, the extraction of the ISW pattern in the SAR image (solid blue curve) is still in the Lombok Strait area with a depth of around 1500 m. Figure 3(b) shows the displacement of three ISW pattern extraction pairs on SGLI, MODIS, and AHI at a depth of around 1500 m. Comparing the movement of ISW patterns in Packet 1 and Packet 2, it is evident that Packet 2 propagates faster than Packet 1, even though both are observed simultaneously. The ISW phase speed estimation results by Tensubam et al. (2021) in the Andaman Sea show that the ISW displacement will decrease when moving from deep to shallow water. Those results are consistent with the SAR and optics estimation results in Packet 1. The average phase speed of ISW Packet 1 is 2.16 m/s in the SAR and SGLI pairs, while the SAR and MODIS pairs propagate with an average phase speed of 2.17 m/s. Additionally, the SAR and AHI pairs experience a slowdown of 0.05 m/s compared to the SGLI and SAR, with an average phase speed of 2.11 m/s.

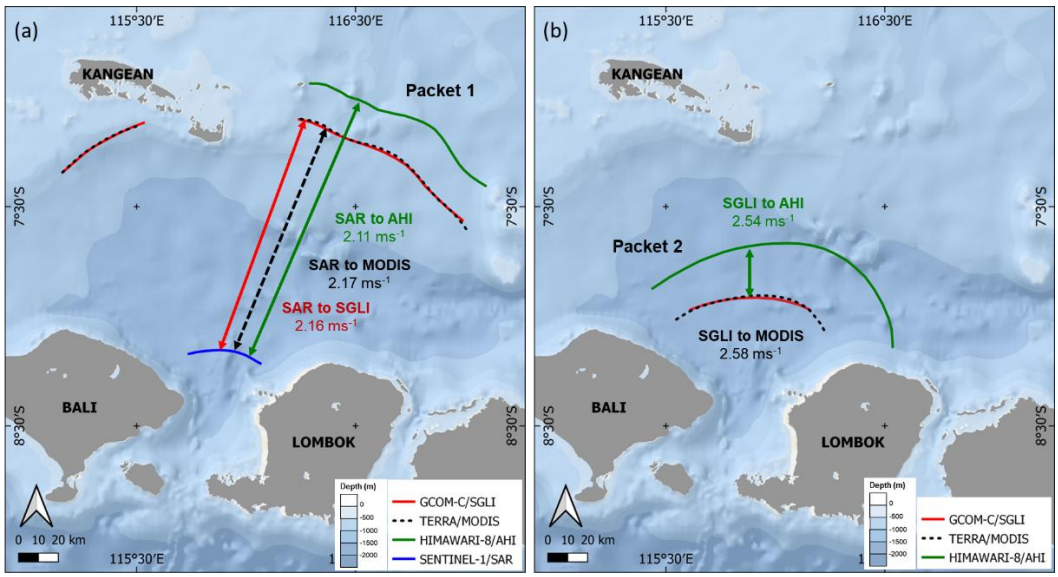

Figure 4. ISW phase speed estimation results (a) Packet 1 using ISW pattern distance and time different from SAR to optical sensors, and (b) Packet 2 using ISW ISW pattern distance and time different from the optical sensor.

In the Lombok Strait, ISW Packet 2 exhibits an average phase speed of 2.58 m/s in the SGLI and MODIS pairs, while SGLI and AHI propagate at an average phase speed of 2.54 m/s. Packet 2's SGLI and AHI pair also experienced a slowdown similar to what in Packet 1. This deceleration was due to AHI being recorded three hours after SGLI and MODIS, causing the ISW extraction to propagate towards shallower waters. The pairing of SGLI and MODIS is exciting because the two ISW extractions almost overlap, thanks to a shorter time difference of four minutes compared to AHI's temporal resolution of ten minutes. In Packet 1, the ISW extraction displacement on SGLI and MODIS over a short time is about 620 m, while in Packet 2, it is about 680 m.

Despite clearer stratification, the ISW phase speed during the southeast monsoon season is slower than during the northwest (Chonnaniyah et al., 2023). Phase speed estimation of ISWs using a single image simultaneously was conducted by analyzing semidiurnal tidal time differences. Sentinel-1/SAR estimated a phase speed of 2.23 m/s, GCOM-C/SGLI 2.12 m/s, Terra/MODIS 2.11 m/s, and the KdV equation 2.15 m/s. The estimation results in this study are consistent with previous research in the Lombok Strait. Purwandana et al. (2021) suggested a phase speed of 1.9 m/s using in-situ data and Himawari-8 imagery, Susanto et al. (2005) using ERS 1/2 reported 1.97-1.99 m/s, and Mitnik et al. (2000) reported phase speeds of 1.8-1.9 m/s using ERS 1/2 SAR images.

4. CONCLUSIONS

ISW phase speed estimation is achieved by comparing pairs of satellite images capturing the same ISW packet at different time intervals. Multi-satellite imagery with closely matched time differences is crucial for accurate phase speed estimation. This study employs various optical sensors, including SGLI, MODIS, and AHI, which capture visible band imagery. The ISW phase speed estimation results, consistent with findings in the Andaman Sea, demonstrate that ISW displacement

decreases as they move from deep to shallow waters. In Package 1, the average phase speed of ISW Packet 1 is 2.16 m/s in the SAR and SGLI pairs, while the SAR and MODIS pairs propagate with an average phase speed of 2.17 m/s. The SAR and AHI pairs experience a slight slowdown of 0.05 m/s compared to the SGLI and SAR pairs, with an average phase speed of 2.11 m/s. ISW Packet 2 exhibits an average phase speed of 2.58 m/s in the SGLI and MODIS pairs, while the SGLI and AHI propagate at an average phase speed of 2.54 m/s. Package 2's SGLI and AHI pair also experienced a similar slowdown, attributed to AHI's delayed recording, causing the ISW extraction to propagate towards shallower waters. Notably, pairing SGLI and MODIS yields results with a shorter time difference, enhancing precision. This research contributes valuable insights into ISW behavior, propagation, and phase speed estimation using multi-satellite imagery. These findings enhance our understanding of oceanic processes and have practical implications for various ecological, climatic, and navigational challenges associated with ISW in the Lombok Strait.

5. ACKNOWLEDGEMENTS

The authors gratefully acknowledge the JSPS RONPAKU Dissertation Ph.D. Program for financial support. Thanks for the data received from the European Space Agency (ESA) and the Copernicus Open Access Hub (previously known as Sentinels Scientific Data Hub) that provides complete, accessible, and open access to Sentinel-1 data (https://scihub.copernicus.eu/). We are grateful to JAXA for the SGLI data that provides free and open access through the Globe Portal System (G-Portal) website (https://gportal.jaxa.jp/gpr/).

6. REFERENCES

Alpers, W., 2014. Ocean Internal Waves. In: *Encyclopedia of Remote Sensing*, edited by Eni G. Njoku, Springer Reference, New York, pp. 433–37.

Apel, J. R., 2002. Oceanic Internal Waves and Solitons. In: *Synthetic Aperture Radar Marine User's Manual*, edited by C. S. Jackson, NOAA/ NESDIS, Washington DC., pp. 189–206.

Bessho, K., Date, K., Hayashi, M., Ikeda, A., Imai, T., Inoue, H., Kumagai, Y., Miyakawa, T., Murata, H., Ohno, T., Okuyama, A., Oyama, R., Sasaki, Y., Shimazu, Y., Shimoji, K., Sumida, Y., Suzuki, M., Taniguchi, H., Tsuchiyama, H., … Yoshida, R. 2016. An Introduction to Himawari-8/9 - Japan's New-Generation Geostationary Meteorological Satellites. *Journal of the Meteorological Society of Japan* 94 (2), pp. 151–83.

Chonnaniyah, Karang, I. W. G. A., & Osawa, T., 2021. Internal Solitary Waves Propagation Speed Estimation in the Northern Part of Lombok Strait Observed by Sentinel-1 SAR and Himawari-8 Images. *IOP Conference Series: Earth and Environmental Science* 944 (1).

Chonnaniyah, Osawa, T., As-Syakur, A. R., Karang, I. W. G. A., & da Silva, J. C. B., 2023. On the Distinction of Seasonal Internal Solitary Waves Characteristics in the Lombok Strait Based on Multi-Satellite Data. *International Journal of Remote Sensing*, pp. 1–16.

Gong, Y., Xie, J., Xu, J., Chen, Z., He, Y., & Cai, S., 2022. Spatial Asymmetry of Non-linear Internal Waves in the Lombok Strait. *Progress in Oceanography* 202 (November 2021), 102759.

Jackson, C., 2007. Internal Wave Detection Using the Moderate Resolution Imaging Spectroradiometer (MODIS). *Journal of Geophysical Research* 112 (C11), C11012.

Jackson, C., da Silva, J., Jeans, G., Alpers, W., & Caruso, M., 2013. Non-linear Internal Waves in Synthetic Aperture Radar Imagery. *Oceanography* 26 (2), pp. 68–79.

Karang, I. W. G. A., Chonnaniyah, C., & Osawa, T., 2019. Landsat 8 Observation of the Internal Solitary Waves in the Lombok Strait. *Indonesian Journal of Geography* 51 (3), pp. 251-260.

Karang, I. W. G. A., & Nishio, F., 2011. Internal Waves in the Lombok Strait Revealed by ALOS PALSAR Images. In *IEEE Intern Geosci.Remote Sensing Symp. IGARSS 2011*, Vancouver, Canada, 17, pp. 253–56.

Liu, B., Yang, H., Ding, X., & Li, X., 2014. Tracking the Internal Waves in the South China Sea with Environmental Satellite Sun Glint Images. *Remote Sensing Letters* 5 (7), pp. 609–18.

Matthews, J. P., Aiki, H., Masuda, S., Awaji, T., & Ishikawa, Y., 2011. Monsoon Regulation of Lombok Strait Internal Waves. *Journal of Geophysical Research: Oceans* 116 (5), pp. 1–14.

Mitnik, L., Alpers, W., & Hock, L., 2000. Thermal Plumes and Internal Solitary Waves Generated in the Lombok Strait Studied by ERS SAR. In *ERS-Envisat Symposium: Looking down to Earth in the New Millenium*, Gothenburg, Sweden: European Space Agency, Publication Division, Noordwijk, The Netherlands, pp. 1–9.

Murray, S. P., Arief, D., Kindle, J. C., & Hurlburt, H. E., 1990. Characteristics of Circulation in an Indonesian Archipelago Strait from Hydrography, Current Measurements and Modeling Results. *The Physical Oceanography of Sea Straits*, pp. 3–4.

Ningsih, N. S., Rahmayani, R., Hadi, S., & Brojonegoro, I. S., 2008. Internal Waves Dynamics in the Lombok Strait Studied By a Numerical Model. *International Journal of Remote Sensing and Earth Sciences* 5, pp. 17–33.

Ogata, K., Toratani, M., & Murakami, H., 2017. GCOM-C/SGLI Level-2 Ocean Color Products Generation. In *2017 IEEE International Geoscience and Remote Sensing Symposium (IGARSS)*, pp. 5648–5649.

Purwandana, A., Cuypers, Y., & Bouruet-Aubertot, P., 2021. Observation of Internal Tides, Non-linear Internal Waves and Mixing in the Lombok Strait, Indonesia. *Continental Shelf Research* 216 (2021): 104358.

Robinson, I. S., 2010. *Discovering the Ocean from Space*. Springer - Praxis Publishing.

Susanto, R. D., Gordon, A. L., & Sprintall, J., 2007. Observations and Proxies of the Surface Layer Throughflow in Lombok Strait. *Journal of Geophysical Research: Oceans* 112 (C03S92), pp. 1–11.

Susanto, R. D., Mitnik, L., & Zheng, Q., 2005. Ocean Internal Waves Observed in the Lombok Strait. *Oceanography* 18 (4), pp. 125–32.

Syamsudin, F., Taniguchi, N., Zhang, C., Hanifa, A. D., Li, G., Chen, M., Mutsuda, H., Zhu, Z. N., Zhu, X. H., Nagai, T., & Kaneko, A., 2019. Observing Internal Solitary Waves in the Lombok Strait by Coastal Acoustic Tomography. *Geophysical Research Letters* 46 (17–18), pp. 10475–10483.

Tensubam, C. M., Raju, N. J., Dash, M. K., & Barskar, H., 2021. Estimation of Internal Solitary Wave Propagation Speed in the Andaman Sea Using Multi–Satellite Images. *Remote Sensing of Environment* 252 (October 2019), 112123.

Woodson, C. B., 2018. The Fate and Impact of Internal Waves in Nearshore Ecosystems. *Annual Review of Marine Science* 10, pp. 421–41.